




# Anisotropic Axisymmetric MHD Equilibria in Spheroidal Coordinates

Leonardo C. Souza<sup>1</sup> · Ricardo L. Viana<sup>1</sup> 

Received: 29 October 2019 / Published online: 28 January 2020  
© Sociedade Brasileira de Física 2020

## Abstract

When subjected to a strong magnetic field, plasmas can exhibit anisotropy in the directions parallel and perpendicular to the field. The magnetohydrodynamics (MHD) equilibrium equation under the hypothesis of Chew, Goldberger, and Low of an anisotropic pressure tensor is solved analytically, using a previously known solution of the isotropic case in oblate spheroidal coordinates. The effects of the anisotropy on the magnetic fields and on the current density are investigated, and the radial profiles of the pressures along and across the magnetic field are studied.

**Keywords** Magnetohydrodynamics · MHD equilibrium · Plasma anisotropy

## 1 Introduction

One of the basic hypotheses of magnetohydrodynamics (MHD) is that collisions among plasma particles are so frequent that it is possible to use a fluid description, i.e., the mean collision time should be very low, compared to a characteristic time of the plasma discharge [1]. However, if the plasma is immersed in a strong magnetic field, as it is often the case in fusion applications, particle gyration with a small Larmor radius can justify a fluid approach, even if the collisionality is not so high as usually required [2].

In this case, the particle motion is quite different along in directions parallel and perpendicular to the strong magnetic field: whereas in the parallel direction we have the fast guiding center motion, in the perpendicular direction the dominant motion is the  $\mathbf{E} \times \mathbf{B}$  drift. Since the latter has the same velocity for both electrons and positive ions, the average kinetic energy will be different in these directions.

This anisotropy under a strong magnetic field has been described by Chew, Goldberger, and Low (CGL) in the form of a diagonal pressure tensor with different components in directions parallel and perpendicular to the field [3]. Using an approximation scheme to solve the corresponding Boltzmann equation, different energy equations have been derived

along parallel and perpendicular directions, the so-called double-adiabatic equations [4]. This approach has been used for a long time in the description of fusion plasmas subjected to heating through neutral-beam injection (NBI), ion cyclotron resonance heating (ICRH), and electron cyclotron resonance heating (ECRH) [5, 6], and also applied to space plasmas, like in the study of the interaction between solar wind and Earth's magnetosheath [7].

The starting point in magnetic confinement theory lies in obtaining physically acceptable ideal MHD equilibria [8]. In the case of asymmetric toroidal configurations, this usually means solving the Grad-Shafranov-Schlüter (GSS) equation in the case of isotropic plasmas [9–11]. The corresponding problem for anisotropic plasmas was first addressed by Mercier and Cotsaftis, who derived a MHD equilibrium equation using the CGL form of the pressure tensor, also studying the MHD stability of the resulting equilibrium configurations [12]. The Mercier-Cotsaftis equation reduces to GSS equation as the plasma becomes isotropic [13].

The Mercier-Cotsaftis equation has been investigated for deriving anisotropic toroidal equilibria both numerically [14–16] and using analytical approximations [17–19]. In 1993, Clemente introduced an integral transform on the flux function which enables us to rewrite the anisotropic Mercier-Cotsaftis equation in the form of a GSS equation [20]. If one knows a solution of the latter, for specified current and pressure profiles, it is formally possible to invert the transformation and obtain a corresponding solution for the anisotropic case. In the same paper, Clemente has obtained a solution for the anisotropic equation for

✉ Ricardo L. Viana  
viana@fisica.ufpr.br

<sup>1</sup> Departamento de Física, Universidade Federal do Paraná,  
81531-990, Curitiba, Paraná, Brazil

cylindrical coordinates starting from a known analytical solution for the isotropic case [21, 22]. Recently, we generalized Clemente's approach for an arbitrary curvilinear coordinate system and applied the formalism to solutions in cylindrical and spherical geometries [23].

Compact toroid configurations, like spheromaks, are an alternative to the tokamak in magnetic confinement research, having the main advantage of not needing external toroidal coils or a toroidal vessel [24]. The oblate configuration (oblimak), of which the spheromak is a limiting case, has been shown to be stable in the MHD limit [25]. For these reasons, the study of the MHD equilibrium in spheroidal-oblate (and closely related prolate) coordinates is of relevance as well as the effects of anisotropy in the magnetic field and current density [26, 27].

Our work can be of interest also for the description of field-reversed configurations (FRC) like the C-2U and C-2W experiments at Tri Alpha Energy, the latter being currently the world's largest FRC device in operation [28, 29]. Such configurations have high beta values (ca 0.9), with poloidal axisymmetric magnetic field, with practically no toroidal component. These machines require only solenoidal coils placed outside a simply connected vacuum vessel, and the edge layer outside of the FRC separatrix provides a natural divertor for magnetic field line exhaustion [28]. The combination of geometry simplicity and high magnetic efficiency makes FRCs interesting configurations for future fusion reactors. In particular, the issue of anisotropic equilibria arises in this context, since the FRC plasma in C-2W is produced by neutral beam injection [29].

In this work, we write down the anisotropic equilibrium equation in spheroidal oblate coordinates by considering suitable representations for quantities like the transversal flux function and current function. We then use the method introduced by Clemente [20] to show how anisotropic solutions can be obtained from a transformation of the isotropic solution, whenever the latter is previously known. With the anisotropic solution, we calculate the radial profiles of the parallel and perpendicular pressures with respect to the local magnetic field direction, and study the effect of anisotropy in the magnetic field and current density of the plasma.

This paper is organized as follows: In Section 2, we present the basic equations of the present model and their form in spheroidal coordinates. Section 3 considers a solution of the isotropic case and its adaptation for anisotropic equilibria through application of the Clemente transform. The properties of the corresponding solution are displayed in Section 4, and the last section is devoted to our conclusions.

## 2 Basic Equations

When subjected to a strong magnetic field, the motion of plasma particles has distinct features along distances parallel and perpendicular to the field. The resulting anisotropy can be characterized by different pressures along parallel and perpendicular directions, denoted by  $p_{\parallel}$  and  $p_{\perp}$ , respectively [3]. The corresponding pressure tensor reads

$$\mathbf{T} = p_{\perp} \mathbf{I} + (p_{\parallel} - p_{\perp}) \frac{\mathbf{B}\mathbf{B}}{B^2}, \quad (1)$$

where  $\mathbf{B}$  is the magnetic field and  $\mathbf{I}$  is the unit tensor, such that the ideal MHD equation of motion (conservation of linear momentum) reads [30]

$$\rho \left[ \frac{\partial \mathbf{V}}{\partial t} + (\mathbf{V} \cdot \nabla) \mathbf{V} \right] = -\nabla \left( p_{\perp} + \frac{B^2}{2\mu_0} \right) + (\mathbf{B} \cdot \nabla) \left[ \frac{\mathbf{B}}{\mu_0} - \frac{p_{\parallel} - p_{\perp}}{B^2} \mathbf{B} \right], \quad (2)$$

where  $\rho$  is the mass density,  $\mathbf{V}$  is the fluid velocity, and  $\mu_0$  is the vacuum magnetic permeability (MKSA units are used). The parallel and perpendicular pressures satisfy the so-called double-adiabatic equations [4]

$$\frac{d}{dt} \left( \frac{p_{\parallel} B^2}{\rho^3} \right) = 0, \quad (3)$$

$$\frac{d}{dt} \left( \frac{p_{\perp}}{\rho B} \right) = 0, \quad (4)$$

which play the role of energy conservation equations in the CGL theory.

The set of ideal MHD equations describing static equilibria are thus the  $\mathbf{V} = \mathbf{0}$  limit of the equation of motion (2) as well as Ampère's law and the magnetic Gauss' law:

$$\nabla \cdot \mathbf{T} = \mathbf{J} \times \mathbf{B}, \quad (5)$$

$$\nabla \times \mathbf{B} = \mu_0 \mathbf{J}, \quad (6)$$

$$\nabla \cdot \mathbf{B} = 0, \quad (7)$$

where  $\mathbf{J}$  is the current density. In the presence of gravitational and stationary rotation, it would be necessary to include also the double adiabatic (3)–(4), situations which are not considered in the present paper, but which have been already investigated [31–33].

From these equations, there follows that

$$\nabla p_{\perp} + \frac{1}{\mu_0} \mathbf{B}(\mathbf{B} \cdot \nabla \sigma_-) + \frac{1}{\mu_0} \sigma (\mathbf{B} \cdot \nabla) \mathbf{B} = \frac{1}{\mu_0} (\nabla \times \mathbf{B}) \times \mathbf{B}, \quad (8)$$

where we defined the anisotropy factor

$$\sigma_- = \frac{p_{\parallel} - p_{\perp}}{|\mathbf{B}|^2 / \mu_0}. \quad (9)$$

It will be convenient to introduce the quantity

$$\bar{p} = \frac{1}{2}(p_{\parallel} + p_{\perp}), \quad (10)$$

which should not be confused with the usual average pressure which, in the anisotropic case, is [20]

$$\langle p \rangle = \frac{1}{3} \text{Tr} \mathbf{T} = \frac{1}{3} (2p_{\perp} + p_{\parallel}). \quad (11)$$

Axisymmetric anisotropic MHD equilibria can be described in a general framework using curvilinear coordinates, which enables us to readily adapt the equations to a convenient coordinate system, depending on the boundary conditions required. Let us consider contravariant coordinates  $(x^1, x^2, x^3)$  for a system described by the contravariant metric tensor  $g^{ij} = \hat{\mathbf{e}}^i \cdot \hat{\mathbf{e}}^j$ , where  $\hat{\mathbf{e}}^i = \nabla x^i$  are contravariant basis vectors. We suppose the existence of an ignorable coordinate  $0 \leq x^3 \leq L$ , such that physical quantities like pressure and magnetic field do not depend on  $x^3$  in axisymmetric configurations.

Considering a coordinate surface  $x^2 = \text{const.}$  and the annulus  $S_2$  bounded by the magnetic axis and a coordinate curve  $x^3$ , the transversal flux function can be defined as the magnetic flux through  $S_2$  per unit length in the  $x^3$  direction [34]

$$\Psi(x^1, x^2) = \frac{1}{L} \int_a^{x^1} dx'^1 \int_0^L dx^3 \sqrt{g} B^2, \quad (12)$$

where  $g = \det(g_{ij})$  and  $x^1 = a$  denote the magnetic axes. Similarly, we define a transverse current flux in terms of the total electric current flowing through the surface  $S_2$  per unit length

$$I(x^1, x^2) = I_{\text{axis}} + \frac{1}{L} \int_a^{x^1} dx'^1 \int_0^L dx^3 \sqrt{g} J^2, \quad (13)$$

where  $I_{\text{axis}} = I(x^1 = a, x^2)$ . In terms of these quantities, the magnetic field and current density can be written as [36]

$$\mathbf{B} = \frac{\hat{\mathbf{e}}_3}{g_{33}} \times \nabla \Psi - \mu_0 I \frac{\hat{\mathbf{e}}_3}{g_{33}}, \quad (14)$$

$$\mathbf{J} = \frac{\hat{\mathbf{e}}_3}{g_{33}} \times \nabla I + J_3 \frac{\hat{\mathbf{e}}_3}{g_{33}}. \quad (15)$$

Taking the dot product of (14) with  $\nabla \Psi$ , we have  $\mathbf{B} \cdot \nabla \Psi = 0$ ; i.e.,  $\Psi(x^1, x^2)$  is a surface function. There follows that any surface function  $f$  is of the general form  $f(\Psi(x^1, x^2))$ . Calculating the right side of (5) and taking the dot product with  $\mathbf{B}$  yields  $\mathbf{B} \cdot \nabla I = 0$ ; i.e.,  $I = I(\Psi)$  is also a surface quantity, hence

$$\mathbf{J} \times \mathbf{B} = -\frac{1}{g_{33}} \left[ \frac{1}{\mu_0} \Delta^* \Psi - I \mathcal{D} + \frac{1}{2} \mu_0 (I^2)' \right] \nabla \Psi. \quad (16)$$

where the prime denotes differentiation with respect to  $\Psi$  and in which we defined the Shafranov operator [34]

$$\Delta^* \Psi = \frac{g_{33}}{\sqrt{g}} \left\{ \frac{\partial}{\partial x^1} \left[ \frac{\sqrt{g}}{g_{33}} \left( g^{11} \frac{\partial \Psi}{\partial x^1} + g^{12} \frac{\partial \Psi}{\partial x^2} \right) \right] + \frac{\partial}{\partial x^2} \left[ \frac{\sqrt{g}}{g_{33}} \left( g^{12} \frac{\partial \Psi}{\partial x^1} + g^{22} \frac{\partial \Psi}{\partial x^2} \right) \right] \right\}, \quad (17)$$

and

$$\mathcal{D} = \frac{g_{33}}{\sqrt{g}} \left[ \frac{\partial}{\partial x^1} \left( \frac{g_{23}}{g_{33}} \right) - \frac{\partial}{\partial x^2} \left( \frac{g_{13}}{g_{33}} \right) \right]. \quad (18)$$

which vanishes identically for orthogonal coordinate systems.

Mercier and Cotsaftis assumed that both  $\sigma_-$  and  $\bar{p}$  should be surface functions, i.e. [12]

$$\bar{p} = \bar{p}(\Psi) \Rightarrow \nabla \bar{p} = \bar{p}' \nabla \Psi, \quad (19)$$

$$\sigma_- = \sigma_-(\Psi) \Rightarrow \nabla \sigma_- = \sigma_-' \nabla \Psi, \quad (20)$$

where the primes denote differentiation with respect to  $\Psi$ . Note that  $\langle p \rangle$ , given by (11) is not a surface function. Moreover, (19) may be the only possibility compatible with configurations in which the boundary surface is a rigid and conducting wall [20]. Using this information in (8), we have

$$\left( \bar{p}' - \frac{B^2}{2\mu_0} \sigma_-' \right) \nabla \Psi = (1 - \sigma_-) \mathbf{J} \times \mathbf{B}. \quad (21)$$

Now substituting (16) for the Lorentz force into the above equation, there results an anisotropic equilibrium equation written in terms of surface quantities only

$$\begin{aligned} \Delta^* \Psi - \mu_0 I \mathcal{D} - \frac{\sigma_-'}{2(1 - \sigma_-)} |\nabla \Psi|^2 \\ = -\frac{1}{2(1 - \sigma_-)} [\mu_0^2 I^2 (1 - \sigma_-)]' - \frac{\mu_0 g_{33} \bar{p}'}{1 - \sigma_-}, \end{aligned} \quad (22)$$

In the isotropic limit, we have  $p_{\parallel} = p_{\perp} = p$ , such that  $\sigma = 0$  and  $\bar{p} = p$ , and we recover the usual Grad-Schlüter-Shafranov equation in curvilinear coordinates [34]

$$\Delta^* \Psi - \mu_0 I \mathcal{D} = -\frac{1}{2} \mu_0^2 (I^2)' - \mu_0 g_{33} p'. \quad (23)$$

It is possible to map the anisotropic (22) to a corresponding isotropic (23) by a convenient integral transform introduced by Clemente [20]. Hence, once an equilibrium solution is known for the latter, we can obtain an infinite number of solutions for the anisotropic equation by inverting this transformation. This method was used in cylindrical and spherical coordinates to generate axisymmetric anisotropic equilibria for different profiles of the appropriate surface quantities [20, 23]. The Clemente transformation consists on defining the function

$$U(\Psi) = \int_0^{\Psi} d\Phi \sqrt{1 - \sigma_-(\Phi)}, \quad (24)$$

such that it is necessary that  $\sigma_- < 1$  which, incidentally, also satisfies one of the local necessary stability criteria derived by Mercier and Cotsaftis [12]. Moreover, in order to avoid other instabilities, it is necessary that  $\sigma > -1$  [20, 37], such that our choices must be so as to respect the condition  $|\sigma_-| < 1$ .

Let us define the new function

$$\mathcal{I} = I\sqrt{1 - \sigma_-}, \quad (25)$$

such that (22), combined with (24), yields [23]

$$\Delta^* U - \mu_0 \mathcal{I} \mathcal{D} = -\frac{1}{2} \mu_0^2 \frac{d\mathcal{I}^2}{dU} - \mu_0 g_{33} \frac{d\bar{p}}{dU}, \quad (26)$$

which is formally identical to (23), provided that  $U \rightarrow \Psi$  and  $\mathcal{I} \rightarrow I$ . The corresponding solution can be found for the anisotropic case by inverting the integral transformation (24), what can only be performed if we make some a priori assumption on the dependence of  $\sigma_-$  with  $\Psi$ . This is equivalent to assume a profile for the surface function  $\sigma_-(\Psi)$ , in the same way as we do with  $\mathcal{I}(\Psi)$  and  $\bar{p}(\Psi)$  to solve (22).

In this work, we will use two different choices, namely

$$\sigma_{-1} = \sigma_0 \Psi_1, \quad (27)$$

$$\sigma_{-2} = \tanh^2(\sigma_0 \Psi_2), \quad (28)$$

where  $\sigma_0$  is a positive constant subjected to the constraints  $|\sigma_{-1,2}| < 1$ . Inserting (27) and (28) into (24), a direct integration yields

$$\Psi_1 = \frac{1}{\sigma_0} \left[ 1 - \left( 1 - \frac{3\sigma_0}{2} U \right)^{2/3} \right], \quad (29)$$

$$\Psi_2 = \frac{2}{\sigma_0} \tanh^{-1} \left[ \tan \left( \frac{\sigma_0 U}{2} \right) \right]. \quad (30)$$

The procedure for deriving axisymmetric anisotropic equilibria is thus as follows: initially, we specify the profiles for the surface functions  $\mathcal{I}(U)$  and  $\bar{p}(U)$ . With them, we write the equilibrium (26) in a given coordinate system, with the appropriate boundary conditions, if any. After solving this equation, we obtain  $U(x^1, x^2)$  and, using (29) or (30) for example, we obtain the desired equilibrium  $\Psi(x^1, x^2)$ .

Once we have  $\Psi$ , the current function is obtained from (25) as well as the “average” pressure  $\bar{p} = \bar{p}(U(\Psi))$ . Both are used to determine  $|\mathbf{B}|^2$  using

$$|\mathbf{B}|^2 = \frac{1}{g_{33}} \left( |\nabla \Psi|^2 + \mu_0^2 I^2 \right). \quad (31)$$

Finally, combining (9) and (10), we have the system

$$p_{\parallel} - p_{\perp} = \frac{1}{\mu_0} |\mathbf{B}|^2 \sigma_-(\Psi), \quad (32)$$

$$p_{\parallel} + p_{\perp} = 2\bar{p}(\Psi), \quad (33)$$

whose solution yields the profiles of  $p_{\parallel}$  and  $p_{\perp}$ .

### 3 Anisotropic Equilibria in Spheroidal Coordinates

A number of configurations of magnetically confined plasmas of the compact torus type, like spheromaks, can be described by prolate spheroids. In the astrophysical context, the equilibrium of fluid masses can be conveniently analyzed by using oblate spheroids. Both coordinate systems are closely related and we first give the necessary formulae for oblate coordinates.

We considered the symmetric axis of the plasma as the  $z$ -axis, such that the oblate spheroidal coordinates ( $x^1 = \xi$ ,  $x^2 = \eta$ ,  $x^3 = \phi$ ) are defined by

$$x = c \cosh \xi \sin \eta \cos \phi, \quad (34)$$

$$y = c \cosh \xi \sin \eta \sin \phi, \quad (35)$$

$$z = c \cosh \xi \cos \eta. \quad (36)$$

where ( $0 \leq \xi \leq \infty$ ,  $0 \leq \eta \leq \pi$ ,  $0 \leq \phi \leq 2\pi$ ) and  $2c$  is the distance between the two foci. Then

$$\sqrt{g} = c^3 (\sinh^2 \xi + \cos^2 \eta) \cosh \xi \sin \eta, \quad (37)$$

and the covariant tensor component is  $g_{33} = c^2 \cosh^2 \eta \sin^2 \eta$ . Since the nondiagonal elements are zero, this is an orthogonal system, such that  $\mathcal{D} = 0$ . It is straightforward to consider prolate spheroidal coordinates by making the transformations  $i \cosh(x) \rightarrow \sinh(x)$ ,  $i \sinh(x) \rightarrow \cosh(x)$  and  $-ic \rightarrow c$  [35].

We assume that the plasma boundary is represented by a spheroid  $\xi = \xi_0$ . The semimajor and semiminor axes are denoted by  $a = c \cosh \xi_0$  and  $b = c \sinh \xi_0$  respectively. Since the axisymmetric surface quantities do not depend on  $\phi$ , the equilibrium equation for the auxiliary function  $U(\xi, \eta)$  is, according to (22) [36]

$$\begin{aligned} & \frac{\partial}{\partial \xi} \left( \frac{1}{\cosh \xi \sin \eta} \frac{\partial U}{\partial \xi} \right) + \frac{\partial}{\partial \eta} \left( \frac{1}{\cosh \xi \sin \eta} \frac{\partial U}{\partial \eta} \right) \\ &= -\frac{c^2 (\sinh^2 \xi + \cos^2 \eta)}{\cosh \xi \sin \eta} \left[ \frac{\mu_0^2}{2} (\mathcal{I}^2)' + \mu_0 c^2 \cosh^2 \xi \sin^2 \eta \bar{p}' \right]. \end{aligned} \quad (38)$$

In order to solve this equation, we need to specify profiles for  $\mathcal{I}$  and  $\bar{p}$  as functions of  $U$ . Let us consider the following profiles

$$\bar{p} = p_0 + \frac{\alpha U}{\mu_0 c^4}, \quad (39)$$

$$\mathcal{I} = \mathcal{I}_0 = \text{const.} \quad (40)$$

where  $p_0$  and  $\alpha$  are positive constants. The solution of the corresponding equilibrium equation has been obtained by Kaneko, Chiyoda, and Hirota and reads [26]

$$U(\xi, \eta) = -\frac{8\alpha U_0}{15} \frac{P'_3(i \sinh \xi_0) \cosh^2 \xi \sin^2 \eta}{\cosh^2 \xi_0 \sinh^2 \xi_0} \left[ 1 - \frac{\cosh \xi}{\cosh \xi_0} + \frac{P'_3(\cos \eta)}{6} \left( \frac{\cosh \xi}{\cosh \xi_0} - \frac{P'_3(i \sinh \xi)}{P'_3(i \sinh \xi_0)} \right) \right] \quad (41)$$

where  $\xi_0 = \tanh^{-1}(b/a)$ ,  $U_0$  is the value of  $U(\xi, \eta)$  at the magnetic axis,  $P_3(x)$  stands for the Legendre polynomial of order 3, and the primes denote differentiation with respect to the argument. A similar solution was considered by Kaneko, Kamitani, and Takimoto to investigate MHD equilibrium and stability of a spheromak with a spheroidal plasma-vacuum interface [27].

With the aid of (29) and (30), and by choosing  $\sigma_0 = 1/(2U_0\alpha)$ , it is possible to invert the Clemente transform so as to obtain the corresponding anisotropic solutions. In Fig. 1, we display the flux contours corresponding to  $u = \text{const.}$  solutions (dashed curve),  $\psi_1 = \text{const.}$  (dot-dashed curve) and  $\psi_2 = \text{const.}$  (solid curve), where  $u = \sigma_0 U$ ,  $\psi_1 = \sigma_0 \Psi_1$  and  $\psi_2 = \sigma_0 \Psi_2$ . Since  $U = U(\Psi)$ , the magnetic axis position

$$r_{\text{axis}} = \frac{\cosh \xi_0}{\sqrt{2}}, \quad z_{\text{axis}} = 0$$

is the same for both isotropic and anisotropic solutions, hence there are no expected magnetic axis shifts nor bifurcations. The two anisotropic solutions derived from  $U$  have similar characteristics, the corresponding values being the same at the plasma boundary, which has an oblate

spheroidal shape as required. The quantitative differences between the two solutions are most pronounced near the magnetic axis.

Using the anisotropic solution  $\Psi$ , we solved (32)–(33) in order to obtain  $p_{\parallel}$  and  $p_{\perp}$ , whose radial profiles (in the equatorial plane  $\eta = \pi/2$ ) are shown in Fig. 2 for the two choices of  $\sigma_{-}$  used to invert Clemente transform (the subscripts 1 and 2 denote the solutions (29) and (30), respectively). We normalize both pressures using  $p_0 = \alpha^2 U_0 / \mu_0 c^4$ .

For both choices of  $\sigma_{-}$ , it turns out that the parallel pressure is always larger than the perpendicular pressure, except at the separatrix (plasma boundary) and the magnetic axis, where they are equal. This difference is due to the anisotropy caused by an intense magnetic field, for which the motion along field lines is unbounded, whereas the perpendicular motion is strongly constrained, what favors the parallel direction. The different choices of  $\sigma_{-}$  yield different anisotropic equilibria but with similar qualitative properties.

From (14) and (15), we calculated the magnetic field and current density, respectively. The radial components  $B_{\xi}$  and  $J_{\xi}$  are both zero at the equatorial plane ( $\eta = \pi/2$ ). In Fig. 3a, we show the radial profile of the poloidal field  $B_{\eta}$  at the equatorial plane, normalized to the quantity  $B_0 = \alpha U_0 / c^2 = \mu_0 \mathcal{I}_0 / c$ . As in Fig. 1, we use dashed lines to indicate the isotropic solution, whereas full and dot-dashed lines are used for anisotropic solutions using the two different choices for  $\sigma_{-}$ . In both cases, there is a field reversal at the magnetic axis position, the solution (30) being closer to the isotropic solution, but with the same essential features. The toroidal field  $B_{\phi}$  is depicted in Fig. 3b, showing no sign reversals and approaching

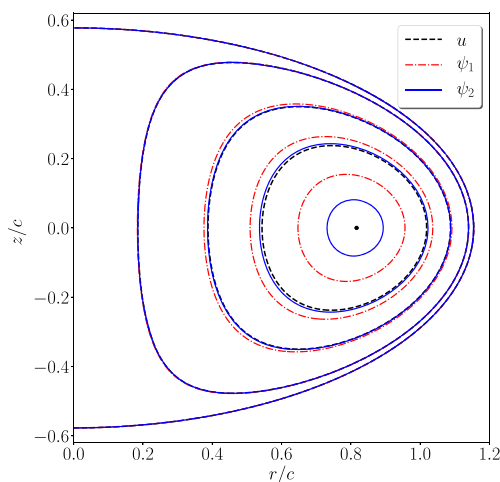


**Fig. 1** (color online) Constant flux contours corresponding to the isotropic solution (black dashed curve), and two anisotropic solutions obtained from it, with  $\sigma_{-1}$  (red dot-dashed curve) and  $\sigma_{-2}$  (blue solid curve). The plasma boundary is an oblate spheroid with  $b/a = 1/2$

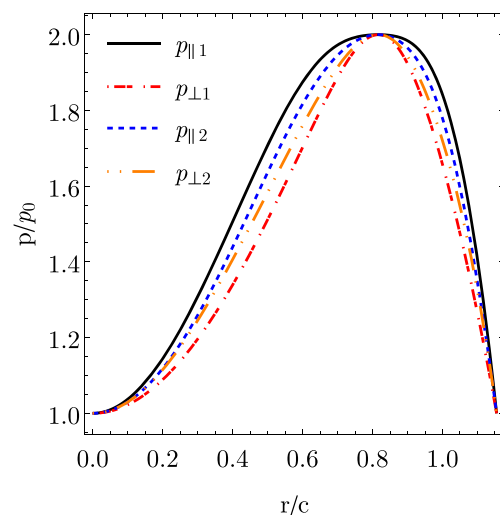
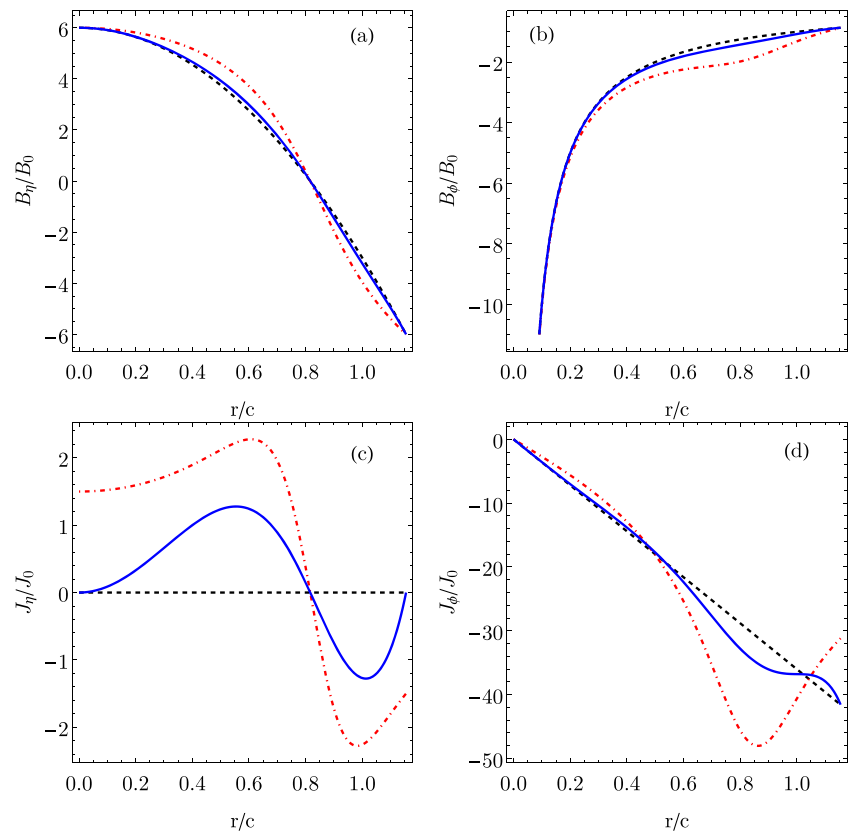


**Fig. 2** (color online) Radial profile of the normalized parallel (solid and dashed) and perpendicular (dot-dashed) pressures, for the two choices of  $\sigma_{-}$  and  $b/a = 1/2$



**Fig. 3** (color online) Radial profiles (in the equatorial plane) for **a** poloidal field, **b** toroidal field, **c** poloidal current, and **d** toroidal current. Dashed lines are used for the isotropic case, and dot-dashed and full lines for the two anisotropic solutions obtained



zero at the plasma boundary. We see again that (30) provides a solution closer to the isotropic case, whereas (29) shows slight differences for  $r/c$  between 0.4 and 1.1, approximately.

The radial profiles of the corresponding poloidal and toroidal current densities are depicted in Fig. 3c and d, respectively, normalized by  $J_0 = I_0/c^2$ . In this case, the anisotropy creates a poloidal current which does not exist in the isotropic case, presenting a sign reversal at the magnetic axis, which leads to a similar change for the corresponding magnetic field. The toroidal current density component has a curious behavior: in the isotropic case, it is monotonically decreasing towards the plasma boundary in a practically linear fashion. The anisotropic solutions, on the other hand, exhibit a nonmonotonic behavior, especially in the vicinity of the magnetic axis. In particular, one of the solutions increases near the boundary, whereas the other decreases like its isotropic counterpart.

## 4 Conclusions

Anisotropic effects are expected in both fusion and astrophysical plasmas when strong magnetic fields are present. The existence of ideal MHD equilibria with axisymmetry

and anisotropic effects (using CGL pressure tensor) has been long recognized, but the corresponding equation is relatively difficult to solve. When the hypotheses (19)–(20) are satisfied, it is possible to introduce an integral transform which maps the anisotropic equilibrium equation into an isotropic one. If a solution of the latter is known, it is possible to obtain an infinite number of anisotropic solutions by inverting this transformation, what requires an additional hypothesis.

In the isotropic version of the MHD equilibrium equation (Grad-Schlüter-Shafranov), it is necessary to specify the pressure profile  $p(\Psi)$ . The anisotropic version of the equilibrium equation, according to the CGL pressure tensor, introduces two different pressures, namely  $p_\perp$  and  $p_\parallel$ , which doubles the number of profiles needed. Instead of specifying profiles for them, in (19)–(20), we rather specify profiles for  $\sigma_-$  and  $\bar{p}$ , which are actually linear combinations of  $p_\perp$  and  $p_\parallel$ .

In this paper, we applied this methodology to axisymmetric toroidal equilibria described by oblate spheroidal coordinates. We start from an analytical solution derived by Kaneko et al. [26, 27] and used two different functions to invert the integral transform, obtaining two different anisotropic equilibria with oblate spheroidal boundary. A simple transformation enables one to consider prolate

spheroids as well. We also consider the latter possibility, but the results were essentially the same as for oblate spheroids.

Our two choices for the anisotropic equilibria produce similar results: the pressure in the direction parallel to the magnetic field is always larger than that in the perpendicular direction, except at the plasma boundary and magnetic axis. This is a natural consequence of the different behaviors of gyrating particles in both directions: strong magnetic fields lead to small Larmor radii, which constrains perpendicular motion, whereas the parallel motion is unbounded. There is no magnetic axis shift due to anisotropy as well. Our results are in accordance with previous solutions by Clemente [20] and ourselves [23]. The magnetic field components are slightly changed when passing from isotropic to anisotropic solutions, but the poloidal current density exhibits a signal reversal in the anisotropic case (for both solutions considered) which is absent in the isotropic case.

It would be possible, for example, to make a modelling of FRCs using the type of solutions developed in this work. For example, Clemente [20] has used a Hill vortex model in order to describe a FRC plasma with ellipsoidal separatrix with semi-axes  $a$  and  $b$  [38]. Our solution, on the other way, has just one parameter, namely  $\xi_0 = \tanh^{-1}(b/a)$ , which fits the axis ratio.

The efforts to obtain analytical solutions of anisotropic equilibria are worth from two points of view. Firstly these solutions can be used for benchmarking computer codes to solve equilibrium equation. Moreover, analytical solutions are always helpful for parametric studies of MHD stability and transport. The relative freedom in choosing the anisotropic equilibrium makes this method a powerful tool to generate such analytical solutions.

**Funding Information** This work has been financially supported by grants from CNPq (Brazilian Government Agency).

## References

1. D.R. Nicholson, *Introduction to Plasma Theory* (Wiley, New York, 1983)
2. H.J. Lee, *Fundamentals of Plasma Physics* (World Scientific, Singapore, 2019)
3. G.F. Chew, M.L. Goldberger, F.E. Low, *Proc. R. Soc. London* **236**, 112 (1956)
4. R.M. Kulsrud, MHD Description of Plasma in *Handbook of Plasma Physics*, vol. I, ch. 1.4, ed. by M.N. Rosenbluth, R.Z. Sagdeev (Publishing Company, North-Holland, 1983)
5. V.D. Pustovitov, *Plasma Phys. Contr. Fusion* **52**, 065001 (2010)
6. A. Fasoli et al., *Nucl. Fusion* **47**, S264 (2007)
7. N.V. Erkaev, H.K. Biernat, D.F. Vogl, C.J. Farrugia, *Adv. Space Res.* **28**, 873 (2001)
8. J.P. Freidberg, *Rev. Mod. Phys.* **54**, 801 (1982)
9. H. Grad, H. Rubin, Hydromagnetic equilibria and force-free fields. in *Proceedings of the 2nd UN Conf. on the Peaceful Uses of Atomic Energy*, Vol. 31 (IAEA, Geneva, 1958), p. 190
10. R. Lüst, A. Schlüter, *Z. Naturforschung* **12a**, 85 (1957)
11. V.D. Shafranov, Plasma equilibrium in a magnetic field. in *Reviews of Plasma Physics*, ed. by M.A. Leontovich, Vol. 2 (Consultants Bureau, New York, 1966)
12. C. Mercier, M. Cotsaftis, *Nucl. Fusion* **1**, 121 (1961)
13. H. Grad, *Phys. Fluids* **10**, 137 (1967)
14. A. Sestero, A. Taroni, *Nucl. Fusion* **16**, 164 (1976)
15. W.A. Cooper et al., *Nucl. Fusion* **20**, 985 (1980)
16. W.A. Cooper, *Phys. Fluids* **26**, 1830 (1983)
17. P.J. Fielding, F.A. Haas, *Nucl. Fusion* **19**, 855 (1979)
18. E.R. Salberta et al., *Phys. Fluids* **30**, 2796 (1987)
19. H.M. Rizk, *J. Plasma Phys.* **38**, 209 (1987)
20. R.A. Clemente, *Nucl. Fusion* **33**, 963 (1993)
21. E.K. Maschke, *Plasma Phys.* **15**, 535 (1973)
22. F. Hernegger, in *Controlled Fusion and Plasma Physics (Proc. 5th Eur. Conf. Grenoble, 1972)*, Vol. 1 (Centre d'Études Nucléaires, Grenoble, 1972), p. 26
23. L.C. Souza, R.L. Viana, *Phys. Plasmas* **26**, 042502 (2019)
24. T.R. Jarboe, *Plasma Phys. Contr. Fusion* **36**, 945 (1984)
25. M.N. Rosenbluth, M.N. Bussac, *Nucl. Fusion* **19**, 489 (1979)
26. S. Kaneko, K. Chiyoda, I. Hirota, *J. Phys. Soc. Japan* **52**, 2016 (1983)
27. S. Kaneko, A. Kamitani, A. Takimoto, *J. Phys. Soc. Japan* **54**, 3347 (1985)
28. H. Gota et al., *Nucl. Fusion* **57**, 116021 (2017)
29. H. Gota et al., *Nucl. Fusion* **59**, 112009 (2019)
30. J.A. Bittencourt, *Fundamentals of Plasma Physics*, 3rd edn. (Springer, New York, 1994)
31. R.A. Clemente, *Plasma Phys. Contr. Fusion* **36**, 707 (1994)
32. R.A. Clemente, R.L. Viana, *Plasma Phys. Contr. Fusion* **41**, 567 (1999)
33. R.A. Clemente, R.L. Viana, *Braz. J. Phys.* **29**, 457 (1999)
34. J.W. Edenstrasser, *J. Plasma Phys.* **24**, 299 (1980)
35. P.M. Morse, H. Feshbach, *Methods of Theoretical Physics*, vol. II, ch. 10 (McGraw-Hill, New York, 1953)
36. R.L. Viana, *Int. J. Theor. Phys.* **37**, 2657 (1998)
37. H. Grad, in *Magneto-Fluid and Plasma Dynamics Symposia in Applied Mathematics*, Vol. 18 (American Mathematical Society, Providence, 1967), p. 162
38. S.P. Auerbach, W.C. Condit, *Nucl. Fusion* **21**, 927 (1981)

**Publisher's Note** Springer Nature remains neutral with regard to jurisdictional claims in published maps and institutional affiliations.